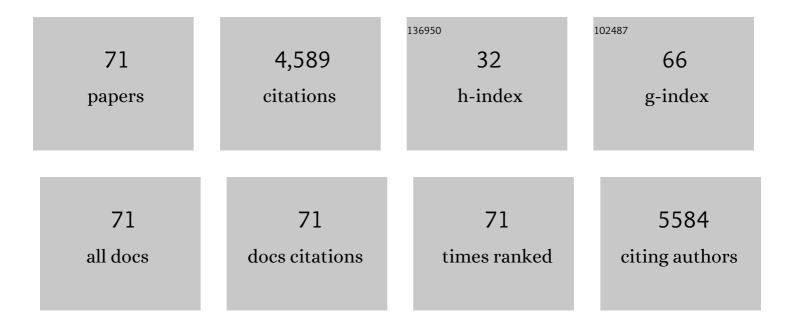
## **Guo-Liang Chai**

List of Publications by Year in descending order

Source: https://exaly.com/author-pdf/8996499/publications.pdf

Version: 2024-02-01



#	Article	IF	CITATIONS
1	Interfacial effects in CuO/Co <sub>3</sub> O <sub>4</sub> heterostructures enhance benzene catalytic oxidation performance. Environmental Science: Nano, 2022, 9, 781-796.	4.3	13
2	In-situ electrochemical modification of pre-intercalated vanadium bronze cathodes for aqueous zinc-ion batteries. Science China Materials, 2022, 65, 1165-1175.	6.3	18
3	Progress, Advantages, and Challenges of Topological Material Catalysts. Small Science, 2022, 2, .	9.9	23
4	Density functional theory study of CH4 dissociation and C C coupling on W-terminated WC(0001) surface. Applied Surface Science, 2022, 591, 153128.	6.1	5
5	Rhodium-based bidentate phosphorus ligand catalyst for direct synthesis of ethylene glycol. Molecular Catalysis, 2022, 524, 112288.	2.0	0
6	Recent progress of Bi-based electrocatalysts for electrocatalytic CO <sub>2</sub> reduction. Nanoscale, 2022, 14, 7957-7973.	5.6	35
7	Pyrimidine-assisted synthesis of S, N-codoped few-layered graphene for highly efficient hydrogen peroxide production in acid. Chem Catalysis, 2022, 2, 1450-1466.	6.1	7
8	Effective Ensemble of Pt Single Atoms and Clusters over the (Ni,Co)(OH) <sub>2</sub> Substrate Catalyzes Highly Selective, Efficient, and Stable Hydrogenation Reactions. ACS Catalysis, 2022, 12, 8104-8115.	11.2	20
9	Regulable pyrrolic-N-doped carbon materials as an efficient electrocatalyst for selective O <sub>2</sub> reduction to H <sub>2</sub> O <sub>2</sub> . New Journal of Chemistry, 2022, 46, 14510-14516.	2.8	7
10	Space onfined One‧tep Growth of 2D MoO <sub>2</sub> /MoS <sub>2</sub> Vertical Heterostructures for Superior Hydrogen Evolution in Alkaline Electrolytes. Small, 2022, 18, .	10.0	20
11	Solvent-mediated engineering of copper-metalated acetylenic polymer scaffolds with enhanced photoelectrochemical performance. Journal of Materials Chemistry A, 2021, 9, 9729-9734.	10.3	5
12	Alleviation of Dendrite Formation on Zinc Anodes via Electrolyte Additives. ACS Energy Letters, 2021, 6, 395-403.	17.4	340
13	Palladium alloys used as electrocatalysts for the oxygen reduction reaction. Energy and Environmental Science, 2021, 14, 2639-2669.	30.8	158
14	LaSiP <sub>3</sub> and LaSi <sub>2</sub> P <sub>6</sub> : Two Excellent Rareâ€Earth Pnictides with Strong SHG Responses as Mid―and Farâ€Infrared Nonlinear Optical Crystals. Advanced Optical Materials, 2021, 9, 2002176.	7.3	9
15	Weakening Intermediate Bindings on CuPd/Pd Core/shell Nanoparticles to Achieve Pt‣ike Bifunctional Activity for Hydrogen Evolution and Oxygen Reduction Reactions. Advanced Functional Materials, 2021, 31, 2100883.	14.9	68
16	Enhancing Hydrogen Evolution Electrocatalytic Performance in Neutral Media via Nitrogen and Iron Phosphide Interactions. Small Science, 2021, 1, 2100032.	9.9	24
17	Conductive Twoâ€Ðimensional Phthalocyanineâ€based Metal–Organic Framework Nanosheets for Efficient Electroreduction of CO <sub>2</sub> . Angewandte Chemie - International Edition, 2021, 60, 17108-17114.	13.8	213
18	Facet Engineering to Regulate Surface States of Topological Crystalline Insulator Bismuth Rhombic Dodecahedrons for Highly Energy Efficient Electrochemical CO <sub>2</sub> Reduction. Advanced Materials, 2021, 33, e2008373.	21.0	84

**GUO-LIANG CHAI** 

#	Article	IF	CITATIONS
19	Conductive Twoâ€Dimensional Phthalocyanineâ€based Metal–Organic Framework Nanosheets for Efficient Electroreduction of CO <sub>2</sub> . Angewandte Chemie, 2021, 133, 17245-17251.	2.0	48
20	Facile Fabrication of Robust Hydrogen Evolution Electrodes under High Current Densities via Pt@Cu Interactions. Advanced Functional Materials, 2021, 31, 2105579.	14.9	45
21	Ba <sub>4</sub> GeSb <sub>2</sub> Se <sub>11</sub> : An Infrared Nonlinear Optical Crystal with a V-Shaped Se <sub>3</sub> <sup>2–</sup> Group Possessing a Large Contribution to the SHG Response. Inorganic Chemistry, 2021, 60, 15593-15598.	4.0	5
22	BaCdGeSe4: Synthesis, structure and nonlinear optical properties. Journal of Solid State Chemistry, 2021, 302, 122352.	2.9	3
23	Highly Selective CO <sub>2</sub> Electroreduction to CH <sub>4</sub> by Inâ€Situ Generated Cu <sub>2</sub> O Singleâ€Type Sites on a Conductive MOF: Stabilizing Key Intermediates with Hydrogen Bonding. Angewandte Chemie, 2020, 132, 23849-23856.	2.0	70
24	Electrochemical oxygen reduction for H <sub>2</sub> O <sub>2</sub> production: catalysts, pH effects and mechanisms. Journal of Materials Chemistry A, 2020, 8, 24996-25016.	10.3	94
25	Acidic Electrolytes: Highâ€Performance Metalâ€Free Nanosheets Array Electrocatalyst for Oxygen Evolution Reaction in Acid (Adv. Funct. Mater. 31/2020). Advanced Functional Materials, 2020, 30, 2070210.	14.9	1
26	A universal pH range and a highly efficient Mo <sub>2</sub> C-based electrocatalyst for the hydrogen evolution reaction. Journal of Materials Chemistry A, 2020, 8, 19879-19886.	10.3	50
27	Highly Selective CO <sub>2</sub> Electroreduction to CH <sub>4</sub> by Inâ€Situ Generated Cu <sub>2</sub> O Singleâ€Type Sites on a Conductive MOF: Stabilizing Key Intermediates with Hydrogen Bonding. Angewandte Chemie - International Edition, 2020, 59, 23641-23648.	13.8	335
28	Frontispiece: Highly Selective CO <sub>2</sub> Electroreduction to CH <sub>4</sub> by Inâ€Situ Generated Cu <sub>2</sub> O Singleâ€īype Sites on a Conductive MOF: Stabilizing Key Intermediates with Hydrogen Bonding. Angewandte Chemie - International Edition, 2020, 59, .	13.8	1
29	Frontispiz: Highly Selective CO <sub>2</sub> Electroreduction to CH <sub>4</sub> by Inâ€Situ Generated Cu <sub>2</sub> O Singleâ€Type Sites on a Conductive MOF: Stabilizing Key Intermediates with Hydrogen Bonding. Angewandte Chemie, 2020, 132, .	2.0	0
30	Mesoporous Carbon Hollow Spheres as Efficient Electrocatalysts for Oxygen Reduction to Hydrogen Peroxide in Neutral Electrolytes. ACS Catalysis, 2020, 10, 7434-7442.	11.2	123
31	Highâ€Performance Metalâ€Free Nanosheets Array Electrocatalyst for Oxygen Evolution Reaction in Acid. Advanced Functional Materials, 2020, 30, 2003000.	14.9	55
32	Defected vanadium bronzes as superb cathodes in aqueous zinc-ion batteries. Nanoscale, 2020, 12, 20638-20648.	5.6	61
33	Integration of Strong Electron Transporter Tetrathiafulvalene into Metalloporphyrin-Based Covalent Organic Framework for Highly Efficient Electroreduction of CO <sub>2</sub> . ACS Energy Letters, 2020, 5, 1005-1012.	17.4	180
34	Template-free synthesis of graphene-like carbons as efficient carbocatalysts for selective oxidation of alkanes. Green Chemistry, 2020, 22, 1291-1300.	9.0	33
35	Ba <sub>6</sub> In <sub>6</sub> Zn <sub>4</sub> Se <sub>19</sub> : a high performance infrared nonlinear optical crystal with [InSe <sub>3</sub> ] <sup>3â^²</sup> trigonal planar functional motifs. Journal of Materials Chemistry C, 2020, 8, 7947-7955.	5.5	15
36	Cobalt single-atoms anchored on porphyrinic triazine-based frameworks as bifunctional electrocatalysts for oxygen reduction and hydrogen evolution reactions. Journal of Materials Chemistry A, 2019, 7, 1252-1259.	10.3	152

**GUO-LIANG CHAI** 

#	Article	IF	CITATIONS
37	Reversible two-channel mechanochromic luminescence for a pyridinium-based white-light emitter with room-temperature fluorescence–phosphorescence dual emission. Physical Chemistry Chemical Physics, 2019, 21, 14728-14733.	2.8	24
38	Ba10In6Zn7S10Se16 and Ba10In6Zn7Se26: Two new infrared nonlinear optical materials with T2 super tetrahedron. Journal of Alloys and Compounds, 2019, 797, 356-362.	5.5	4
39	Effect of Axial Coordination of Iron Porphyrin on Their Nanostructures and Photocatalytic Performance. Crystal Growth and Design, 2019, 19, 3279-3287.	3.0	13
40	Adsorption and migration of alkali metals (Li, Na, and K) on pristine and defective graphene surfaces. Nanoscale, 2019, 11, 5274-5284.	5.6	149
41	Ba10In6Zn7S26-nZnS: An Inorganic Composite System with Interface Phase-Matching Tuned for High-Performance Infrared Nonlinear Optical Materials. Inorganic Chemistry, 2019, 58, 3990-3999.	4.0	8
42	Atom-Resolved Analysis of Birefringence of Nonlinear Optical Crystals by Bader Charge Integration. Journal of Physical Chemistry C, 2019, 123, 31183-31189.	3.1	37
43	Unraveling the Reactivity and Selectivity of Atomically Isolated Metal–Nitrogen Sites Anchored on Porphyrinic Triazine Frameworks for Electroreduction of CO <sub>2</sub> . CCS Chemistry, 2019, 1, 384-395.	7.8	125
44	Theoretical Evaluation on Terahertz Source Generators from Ternary Metal Chalcogenides of PbM <sub>6</sub> Te <sub>10</sub> (M = Ga, In). Journal of Physical Chemistry C, 2018, 122, 4557-4564.	3.1	21
45	PbGa <sub>2</sub> GeS <sub>6</sub> : An Infrared Nonlinear Optical Material Synthesized by an Intermediate-Temperature Self-Fluxing Method. Crystal Growth and Design, 2018, 18, 1162-1167.	3.0	30
46	Copper-surface-mediated synthesis of acetylenic carbon-rich nanofibers for active metal-free photocathodes. Nature Communications, 2018, 9, 1140.	12.8	115
47	Topological phase transitions driven by strain in monolayer tellurium. Physical Review B, 2018, 98, .	3.2	34
48	Fe Vacancies Induced Surface FeO <sub>6</sub> in Nanoarchitectures of Nâ€Doped Graphene Protected βâ€FeOOH: Effective Active Sites for pHâ€Universal Electrocatalytic Oxygen Reduction. Advanced Functional Materials, 2018, 28, 1803330.	14.9	51
49	Thermoelectric properties of two-dimensional selenene and tellurene from group-VI elements. Physical Chemistry Chemical Physics, 2018, 20, 24250-24256.	2.8	73
50	Znâ€MOFâ€74 Derived Nâ€Doped Mesoporous Carbon as pHâ€Universal Electrocatalyst for Oxygen Reduction Reaction. Advanced Functional Materials, 2017, 27, 1606190.	14.9	231
51	Two-Electron Oxygen Reduction on Carbon Materials Catalysts: Mechanisms and Active Sites. Journal of Physical Chemistry C, 2017, 121, 14524-14533.	3.1	89
52	Active sites engineering leads to exceptional ORR and OER bifunctionality in P,N Co-doped graphene frameworks. Energy and Environmental Science, 2017, 10, 1186-1195.	30.8	431
53	Theoretical Evaluation of Terahertz Sources Generated From SnGa <sub>4</sub> Q <sub>7</sub> (Q=S,) Tj ETQq1	1 0.7843 2.1	314 rgBT /O
54	Robust 3D macroporous structures with SnS nanoparticles decorating nitrogen-doped carbon nanosheet networks for high performance sodium-ion batteries. Journal of Materials Chemistry A, 2017, 5, 23460-23470.	10.3	79

**GUO-LIANG CHAI** 

#	Article	IF	CITATIONS
55	Indirect Four-Electron Oxygen Reduction Reaction on Carbon Materials Catalysts in Acidic Solutions. ACS Catalysis, 2017, 7, 7908-7916.	11.2	42
56	Exceptional thermoelectric performance of a "star-like―SnSe nanotube with ultra-low thermal conductivity and a high power factor. Physical Chemistry Chemical Physics, 2017, 19, 23247-23253.	2.8	7
57	Nitrogen-Mediated Graphene Oxide Enables Highly Efficient Proton Transfer. Scientific Reports, 2017, 7, 5213.	3.3	4
58	Highly Efficient Oxygen Reduction Catalysts by Rational Synthesis of Nanoconfined Maghemite in a Nitrogen-Doped Graphene Framework. ACS Catalysis, 2016, 6, 3558-3568.	11.2	74
59	Highly effective sites and selectivity of nitrogen-doped graphene/CNT catalysts for CO <sub>2</sub> electrochemical reduction. Chemical Science, 2016, 7, 1268-1275.	7.4	199
60	Active Sites and Mechanisms for Oxygen Reduction Reaction on Nitrogen-Doped Carbon Alloy Catalysts: Stone–Wales Defect and Curvature Effect. Journal of the American Chemical Society, 2014, 136, 13629-13640.	13.7	273
61	Possible Oxygen Reduction Reactions for Graphene Edges from First Principles. Journal of Physical Chemistry C, 2014, 118, 17616-17625.	3.1	56
62	Reply to the â€~Comment on "Planar tetra-coordinate carbon resulting in enhanced third-order nonlinear optical response of metal-terminated graphene nanoribbonsâ€â€™ by P. Karamanis, N. Otero and C. Pouchan, J. Mater. Chem. C, 2013, DOI: 10.1039/C3TC00922J. Journal of Materials Chemistry C, 2013, 1, 3041.	5.5	2
63	THEORETICAL STUDY OF ONE- AND TWO-PHOTON ABSORPTION PROPERTIES FOR THREE SERIES OF DIPHENYLAMINE AND DIFLUORENYLAMINE SUBSTITUTED CONJUGATED COMPOUNDS. Journal of Theoretical and Computational Chemistry, 2012, 11, 1033-1056.	1.8	3
64	Structure dependent electronic and magnetic properties of graphitic GaN–ZnO nanoribbons. Journal of Materials Chemistry, 2012, 22, 7708.	6.7	6
65	Nonlinear optical properties of carbon nitride nanotubes. Physical Chemistry Chemical Physics, 2012, 14, 835-839.	2.8	17
66	Effect of cage size on the thirdâ€order optical properties of endohedral metallofullerenes Sc <sub>3</sub> N@C <sub>2<i>n</i></sub> (2 <i>n</i> = 68, 70, 78, and 80): A theoretical study. International Journal of Quantum Chemistry, 2012, 112, 759-769.	2.0	4
67	Theoretical study on the oneâ€; twoâ€; and threeâ€photon absorption properties of exohedral functionalized derivative of Sc <sub>3</sub> N@C <sub>80</sub> . International Journal of Quantum Chemistry, 2012, 112, 1198-1208.	2.0	1
68	Planar tetra-coordinate carbon resulting in enhanced third-order nonlinear optical response of metal-terminated graphene nanoribbons. Journal of Materials Chemistry, 2012, 22, 11303.	6.7	24
69	Graphitic GaN–ZnO and corresponding nanotubes. Journal of Materials Chemistry, 2011, 21, 17071.	6.7	5
70	First-principles study of ZnO cluster-decorated carbon nanotubes. Nanotechnology, 2011, 22, 445705.	2.6	13
71	First-principles study of CN carbon nitride nanotubes. Nanotechnology, 2010, 21, 195702.	2.6	19